JOURNAL OF GUIDANCE, CONTROL, AND DYNAMICS
Vol. 29, No. 6, November–December 2006

Tailored Dynamic Gain-Scheduled Control

C. D. C. Jones,* M. H. Lowenberg,† and T. S. Richardson‡
University of Bristol, Bristol, BS8 1TR England, United Kingdom

DOI: 10.2514/1.17295

This paper advances the theoretical basis and application of dynamic gain-scheduled control, a novel method for the control of nonlinear systems, to an aircraft model. Extensions of this method involving multivariable gain scheduling and continuation tailoring are developed. The idea behind this method is to schedule the control law gains with a fast-varying state rather than with a slow-varying state or an input parameter. This approach is advantageous because it is then possible to schedule the gains with a state that is dominant in the mode that we are most interested in controlling. The use of this type of gain scheduling is shown to improve the transient response of the aircraft model when stepping between trim conditions and to reduce control surface movement, thus reducing the potential for saturation problems. Hidden coupling terms that introduce unwanted dynamics when scheduling gains with a fast state (rather than the input design parameter) are eliminated directly by applying a transformation to the classical parameter-scheduled gain distributions that are calculated using optimal control theory. A highly nonlinear unmanned combat air vehicle model is used to demonstrate the design process.

Nomenclature

K	=	static gain
K_{ff}	=	feedforward gain schedule
K_x	=	static gain on x
p	=	body axis roll rate
p_{dem}	=	demanded body axis roll rate
q	=	body axis pitch rate
q_{dem}	=	demanded body axis pitch rate
r	=	body axis yaw rate
$\bar{r}$	=	reference input
u	=	control input
x	=	state
α	=	angle of incidence
α_{dem}	=	demanded angle of incidence
α_{int}	=	α command augmentation system integrator state
β	=	angle of sideslip
β_{dem}	=	demanded angle of sideslip
β_{int}	=	β command augmentation system integrator state
δ_e	=	elevator actuator position
$\delta_{e_{\text{dem}}}$	=	demanded elevator actuator position
δ_{yaw}	=	yaw thrust vectoring effector
μ	=	continuation parameter
ϕ	=	dynamic gain
ϕ_x	=	dynamic gain on x

I. Introduction

GAIN scheduling is defined as the process of subdividing a nonlinear control problem into a series of linear subproblems, designing controllers to suit each linear design condition, and reconstructing the resultant discrete solution into a single continuous controller [1]. This divide-and-conquer approach enables well-established linear design methods to be applied to nonlinear problems. Continuity of the controller with linear design methods is also desirable because they are often the basis of safety certification methods.

There has been an upsurge in gain-scheduling research in the last 15 years. Excellent reviews of much of this work can be found in the survey papers by Rugh and Shamma [2] and Leith and Leithead [3]. The aim of this work has been to relax the restrictions associated with classical gain-scheduling approaches, in particular (according to [3]): the restriction to near equilibrium operation that arises from the use of only equilibrium information (namely, the equilibrium linearizations of the plant) for control design purposes; and the slow variation conditions associated with ensuring that the overall system does not evolve between operating regions in too rapid a manner. The former of these restrictions can be addressed using fuzzy/neural approaches, linear/quasi-linear parameter-varying (LPV) formulations and off-equilibrium linearization [3]. (It should be noted that this restriction is not particular to gain scheduling, but applies to linear models in general). The work presented here focuses on the relaxation of the latter restriction by linearization-based gain scheduling using the novel method of dynamic gain scheduling (DGS).

Apart from linearization-based approaches, the other focus of gain-scheduled controller design research in recent years has been on LPV approaches. For example, Apkarian et al. [4] have applied LPV approaches to the control of a missile model and show that tight robustness and performance specifications can be maintained even for rapidly changing parameters. An LPV H_∞ formulation has also been shown to be very suitable for robust control in practice following flight testing on the vectored-thrust aircraft advanced control (VAAC) Harrier [5]. To retain a reasonable focus to the paper, LPV gain-scheduling approaches (which are less strongly based on divide-and-conquer ideas) are not considered, though it should be noted that by addressing time-varying parameters during the design process itself (as opposed to post-design analysis) LPV approaches have the potential to alleviate the slow variation restriction as well.

This paper addresses gain-scheduled control via the linearization-based method of DGS, which has been defined as [1] "... scheduling gains with one (or more) of the system states while accounting for the 'hidden coupling terms' ensures that the controller gains are always set for the current state-space location and therefore produce a near-optimal response."

Hidden coupling terms (also known as fictitious gains or hidden loops) are additional terms in the actual linearized controller when compared with the designed linear controller [6,7]. Therefore, they alter the intended stability of the closed-loop system and could cause instability. Potential ways of dealing with these terms have been discussed previously in the literature [6–8]. Our approach offers a more general means of dealing with these terms by applying a simple numerical transformation to the classically designed gain-scheduled controller.

Received 1 July 2005; revision received 11 January 2006; accepted for publication 11 January 2006.

*Postgraduate Student, Department of Aerospace Engineering. Member AIAA.

†Senior Lecturer, Department of Aerospace Engineering; M.Lowenberg@bris.ac.uk. Senior Member AIAA.

‡Lecturer, Department of Aerospace Engineering. Member AIAA.

The classical gains are calculated as a series of equilibrium linearizations, hence they should be scheduled with the variable that parameterized the equilibrium points. This parameter could be either a control input or a slowly-varying state such as velocity. It would be more desirable to schedule the gains with a fast-varying state, because it is the fast modes that dominate the aircraft response (slow modes can be easily damped out by the pilot or automatic control system). However, this would have an effect on the closed-loop stability, because state scheduling (as opposed to parameter scheduling) introduces additional terms into the elements of the Jacobian matrix. It is these additional terms that are referred to as hidden coupling terms. Our method accounts for these terms by using dynamic gain schedules that are obtained by applying a transformation to the classical (static) gain schedules.

This type of controller is particularly useful when rapid control inputs are demanded. These could occur, for example, when a pilot is carrying out an evasive maneuver or when the higher level mission controller of a semiautonomous unmanned combat air vehicle (UCAV) requires a sudden change in trajectory that is not restricted by the usual g-limits of piloted aircraft.

The method is applied to the ICE 101-TV [9,10], which was designed by Lockheed Martin Tactical Aircraft Systems, Inc. as part of the innovative control effectors (ICE) program. Its open-loop flight envelope is highly nonlinear, hence the closed-loop gain variation allows for a proper assessment of this control method. It is a tailless delta-wing configuration with a 65 deg leading edge sweep and a sawtooth trailing edge. It has five aerodynamic control surfaces as shown in Fig. 1 [all-moving wing tips (AMT), pitch flaps (PF), leading edge flaps (LEF), elevons (ELEV), and spoiler slot deflectors (SSD)] and a pitch/yaw thrust vectoring capability. (Note that the effector post-fix *act* refers to the actuator that is associated with it, for example, PFact = pitch flap actuator, and the L post-fix refers to the left (port) element of the effector, for example, AMTL = left AMT.) Although the ICE was not specifically designed to be unmanned, its configuration is similar to some current UCAVs [11] and is therefore suitable for manned or unmanned research studies.

Results are presented for a second-order (α and q) longitudinal model with an α-demand (α_{dem}) stability and command augmentation system (SCAS), and two fifth-order (α, β, p, q, and r) longitudinal/lateral models, one with a β-demand (β_{dem}) SCAS and the other with both a β_{dem} and an α_{dem} SCAS. The trim points and static gains are determined together within a continuation design framework [12] using LQR [13,14]. This has the advantage of giving the user explicit knowledge of the closed-loop dynamics throughout parameter space so that a strong link with the underlying physics is retained. State-scheduled dynamic gains are then calculated directly from these parameter-scheduled static gains. Feedfoward gain schedules are also used to compensate for a byproduct of the transformation to dynamic gain schedules when large values of the reference input are encountered. This schedule will be created using continuation tailoring (a subset of bifurcation tailoring that has previously been applied to the control of highly nonlinear aircraft [15,16]).

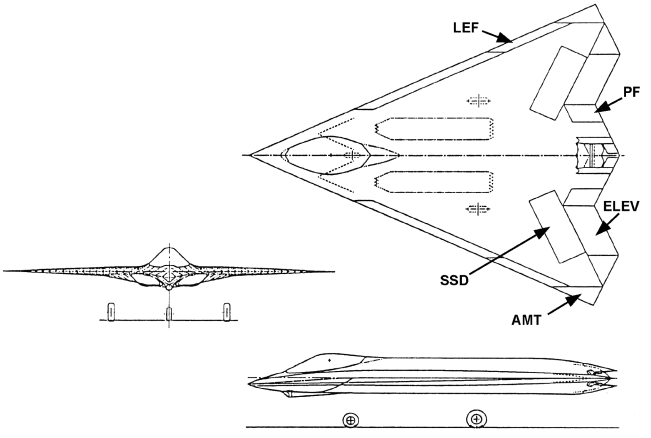

Fig. 1 Schematic drawing of the ICE [9].

II. Methodology/Problem Definition

Following the methodology described in previous work [17] and included here for clarity, first consider the nonlinear system:

$$\dot{\boldsymbol{x}} = \boldsymbol{F}(\boldsymbol{x}, \boldsymbol{\delta}) \tag{1}$$

where

$\boldsymbol{x} \in \Re^n$ = state vector
$\boldsymbol{\delta} \in \Re^p$ = vector of parameters
$\boldsymbol{F}: \Re^{n+p} \to \Re^n$ = smooth nonlinear system

Fixing all elements in $\boldsymbol{\delta}$ apart from one, μ

$$\dot{\boldsymbol{x}} = \boldsymbol{f}(\boldsymbol{x}, \mu) \tag{2}$$

where $\boldsymbol{f}: \Re^{n+1} \to \Re^n$ is a nonlinear system. Adding a nonlinear controller to the system, we obtain

$$\dot{\boldsymbol{x}} = \boldsymbol{g}(\boldsymbol{x}, \mu, \boldsymbol{u}) \tag{3}$$

where $\boldsymbol{u} \in \Re^m$ is a vector of control inputs and $\boldsymbol{g}: \Re^{n+1+m} \to \Re^n$ is a nonlinear system.

Linearizing with μ fixed at an equilibrium point, we obtain

$$\dot{\hat{\boldsymbol{x}}} = \boldsymbol{A}\hat{\boldsymbol{x}} + \boldsymbol{B}\hat{\boldsymbol{u}} \tag{4}$$

$$\hat{\boldsymbol{y}} = \boldsymbol{C}\hat{\boldsymbol{x}} + \boldsymbol{D}\hat{\boldsymbol{u}} \tag{5}$$

where $\hat{\boldsymbol{x}}$ and $\hat{\boldsymbol{u}}$ are perturbations from the linearization point, and $\hat{\boldsymbol{y}}$ is the output vector (also relative to the linearization point). Consider a state-feedback scheme where $\boldsymbol{u}$ is considered in terms of $\boldsymbol{x}$ and an appropriate feedback gain matrix $\boldsymbol{K}$, giving the closed-loop system

$$\dot{\hat{\boldsymbol{x}}} = \boldsymbol{A}\hat{\boldsymbol{x}} + \boldsymbol{B}\boldsymbol{K}\hat{\boldsymbol{x}} = \boldsymbol{A}_{\text{cl}}\hat{\boldsymbol{x}} \tag{6}$$

The gain matrix can then be calculated from the preceding linearization using any convenient method such as LQR, eigenstructure assignment [16–20] or H_∞ [6,21]. This is done quasicontinuously at trim points throughout the μ range by incorporating the linear controller design method within a continuation algorithm[§] (using the AUTO software [22], in this case).

A. Dynamic Gain Scheduling with the Feedback State

The gain matrices can vary considerably between points in state-space for a highly nonlinear system, and so it is necessary to schedule them against either $\boldsymbol{x}$ or μ to maintain the desired control performance.

It is desirable to schedule the gains with a state that is associated with the dominant mode so that the gains can evolve sufficiently quickly during a rapid maneuver. At subsonic speeds it might be preferable to schedule an aircraft control system with angle of incidence α, but in the transonic region it may be more advisable to use the Mach number as the scheduling parameter. In effect, our approach enables an increase in the choice of the scheduling signal, depending on the flight regime.

However, scheduling against $\boldsymbol{x}$ leads to a problem as demonstrated by the following simple example.

Let a second-order aircraft system in α and q (the pitch rate) with state feedback on both states be represented by the following equations of motion:

$$\dot{\alpha} = f_1(\alpha, q) \tag{7}$$

[§]Continuation methods enable the aircraft trim points to be traced out as a function of a system parameter (such as center of gravity position or control surface angle).

$$\dot{q} = f_2(\alpha, q) + K_\alpha(\bar{r})\alpha + K_q(\bar{r})q \tag{8}$$

where $\bar{r}$ is equal to μ for all the cases considered in this paper.

The Jacobian $\boldsymbol{J}$ of this system has the form

$$\boldsymbol{J} = \begin{bmatrix} (\partial\dot{\alpha}/\partial\alpha) & (\partial\dot{\alpha}/\partial q) \\ (\partial\dot{q}/\partial\alpha) & (\partial\dot{q}/\partial q) \end{bmatrix} \tag{9}$$

If the gains are scheduled with $\bar{r}$, then the terms in $\boldsymbol{J}$ become

$$\partial\dot{\alpha}/\partial\alpha = \partial f_1/\partial\alpha \tag{10}$$

$$\partial\dot{\alpha}/\partial q = \partial f_1/\partial q \tag{11}$$

$$\partial\dot{q}/\partial\alpha = (\partial f_2/\partial\alpha) + K_\alpha(\bar{r}) \tag{12}$$

$$\partial\dot{q}/\partial q = (\partial f_2/\partial q) + K_q(\bar{r}) \tag{13}$$

If, however, each gain is scheduled with its feedback state instead of the reference input, that is, $K_\alpha(\alpha)$ and $K_q(q)$, then the terms in $\boldsymbol{J}$ become

$$\partial\dot{\alpha}/\partial\alpha = \partial f_1/\partial\alpha \tag{14}$$

$$\partial\dot{\alpha}/\partial q = \partial f_1/\partial q \tag{15}$$

$$\partial\dot{q}/\partial\alpha = (\partial f_2/\partial\alpha) + K_\alpha(\alpha) + (\partial K_\alpha/\partial\alpha)\alpha \tag{16}$$

$$\partial\dot{q}/\partial q = (\partial f_2/\partial q) + K_q(q) + (\partial K_q/\partial q)q \tag{17}$$

The problem arises because when designing the controller, the gains are calculated at specific reference points, that is, in a static sense, $\partial K_\alpha/\partial\alpha = \partial K_q/\partial q = 0$. When implemented, however, these partial derivatives are not, in general, zero because α and q are dynamically-varying states of the system.

Hence, scheduling against the feedback state rather than with the reference input introduces coupling terms (between dependent and independent schedule variables) that produce unwanted additional dynamics: these are the aforementioned hidden coupling terms. Our approach to minimizing the effect of the coupling terms is to define a different set of gain schedules that retain the same eigenstructure as in the design (static) situation at all reference (trim) conditions.

Therefore, the problem associated with gain scheduling against a state x is to find a nonlinear gain matrix $\phi(x)$, such that the closed-loop system has the same desired eigenstructure as a system that schedules its gains $K(\bar{r})$ with μ. The solution to this problem is most simply explained by example, by considering the following first-order system:

$$\dot{x} = f(x, \mu) + u \tag{18}$$

where $x \in \Re$, $u \in \Re$. Assume we wish to design two controllers of the form $u = K(\bar{r})x$ and $u = \phi(x)x$ by applying LQR to the linearized model at a set of trimmed points. It has been shown in previous work [1] that if the eigenstructures of the two closed-loop systems are to be identical, then the two sets of gains $K(\bar{r})$ and $\phi(x)$ are related by the following equation:

$$K(\bar{r}) = (\partial\phi/\partial x)x + \phi(x) \tag{19}$$

Therefore the dynamic gain schedule (DGS) is given by:

$$\phi(x) = \left[\int K(\bar{r})\,\mathrm{d}x + c\right]/x \tag{20}$$

where c is the constant of integration.[‖]

From this point onwards, if the gains are scheduled with either the reference input $\bar{r}$ or a slowly-varying state, then they are referred to as static gains K. If the gains are instead scheduled with a fast-varying state, then they are referred to as dynamic gains ϕ.

The transformation from static gain K to dynamic gain ϕ can be applied to any nth-order system, provided that each gain is only scheduled against the state to which it is applied. If there is such feedback on any state in any of the n equations, then the transformation in Eq. (20) can be used to find $\phi(x)$ from $K(\bar{r})$. For example,

$$\dot{x}_1 = f(x) + K_1(\bar{r})x_1 + K_2(\bar{r})x_2 \tag{21}$$

can be used to get

$$\dot{x}_1 = f(x) + \phi_1(x_1)x_1 + \phi_2(x_2)x_2 \tag{22}$$

In practice, K will be determined between a lower limit x_l and an upper limit x_u, that is, even though it is defined as a function of μ, because each μ has a corresponding equilibrium value of x, it is effectively a function of trimmed x as well[¶]:

$$K(x_u)x_u = \int_{x_l}^{x_u} K(x)\,\mathrm{d}x + K(x_l)x_l \tag{23}$$

The term $K(x_l)x_l$ is a constant and is zero when the integration is started from zero (i.e., $x_l = 0$). Because we have been using ϕ to define a schedule that is a function of x, we define the state-scheduled gain ϕ as

$$\phi(x_u) = \left[\int_{x_l}^{x_u} K\,\mathrm{d}x + \phi(x_l).x_l\right]/x_u \tag{24}$$

$K(x)$ has been found numerically from the continuation method, and so $\phi(x_u)$ can be calculated via a numerical integration of $K(x)$; trapezoidal integration was used in this work.

Dynamic state-scheduled gains directly account for the coupling terms in the Jacobian matrix, as the DGS is obtained by applying a transformation to the static gain schedule.

Therefore, for the system defined by Eqs. (7) and (8), the dynamic gains can be related to the static gains by simply applying Eq. (19) in the following way:

$$K_q = q(\partial\phi_q/\partial q) + \phi_q(q) \tag{25}$$

$$K_\alpha = \alpha(\partial\phi_\alpha/\partial\alpha) + \phi_\alpha(\alpha) \tag{26}$$

B. Dynamic Gain Scheduling with a State Other than the Feedback State

It is sometimes not possible to convert a static gain schedule to a DGS by simply applying Eq. (20), due to the numerics of the data; for example, when the function relating the trim states x to the gain K is a one-to-many function, or when the state does not go through zero, as this prevents an initial condition for integration being determined exactly. In fact, one of the advantages of the continuation-based approach is that the nature of K throughout parameter space will be immediately apparent. Schematic examples of these problematic data trends are shown in Fig. 2. They are both one-to-many functions for at least some of their state range x_1 and x_2. The second subplot is additionally problematic, as it does not pass through $x_2 = 0$ within the given continuation parameter range. The constant of integration c

[‖]The static gains are calculated at each point along the trim branch. This closed-loop trim branch yields a unique set of points (i.e., one set of gains at each solution point). Hence, integration of K with respect to trimmed x produces a unique curve.

[¶]K is a function of μ, and x is a function of μ. The steady-state continuation provides the link between the two, that is, between K and x at trim conditions over a range of μ inputs; hence, $K(x)$ only has meaning for trim points.

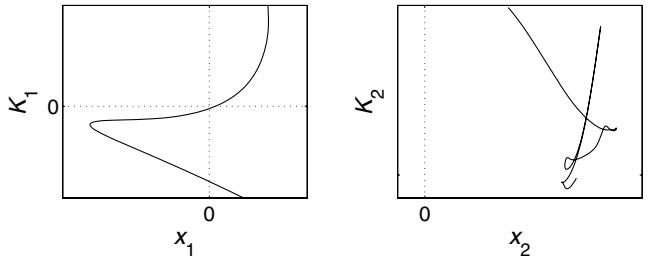

a) Example 1 b) Example 2

Fig. 2 Example problematic data trends.

is equal to the product of ϕ and x, but ϕ is unknown before its transformation from K. Hence, if the integration is started from 0, then c is known. Its complexity also serves to demonstrate why a piecewise transformation process was not attempted. A piecewise process would involve the splitting of the one-to-many function into a series of one-to-one or many-to-one functions, transforming each individually, concatenating the resulting gains, and then necessarily scheduling them with multiple parameters.

In such situations it is possible to schedule with a state other than the feedback state, but the DGS must then be calculated using an alternative transformation. This novel process is referred to as a modified transformation and is best described by the following example:

Consider a third-order closed-loop aircraft system (α, q, and δ_e), where the elevator actuator transfer function relating its δ_e to its $\delta_{e_{\text{dem}}}$ is modeled as a first-order lag of the form $30/(s+30)$:

$$\dot{\alpha} = f_1(\alpha, q, \delta_e) \tag{27}$$

$$\dot{q} = f_2(\alpha, q, \delta_e) \tag{28}$$

$$\dot{\delta}_e = -30\delta_e + 30[K_\alpha(\mu)\alpha + K_q(\mu)q] \tag{29}$$

Now if state-scheduled dynamic gain feedback is required instead of μ-scheduled static gain feedback, then Eq. (29) is replaced by:

$$\dot{\delta}_e = -30\delta_e + 30[\phi_\alpha(\alpha)\alpha + \phi_q(q)q] \tag{30}$$

and the standard transformations can be applied to get the dynamic gains ϕ from the static gains K, which are in this case the same as those given in Eqs. (25) and (26).

This is referred to as a full dynamic gain schedule (F-DGS), that is, all the system gains can be transformed with their associated feedback state.

However, for example, if K_q cannot be transformed to ϕ_q using q because of one of the previously mentioned numerical restrictions, then the $\dot{\delta}_e$ equation may take the following form instead:

$$\dot{\delta}_e = -30\delta + 30[\phi_\alpha(\alpha)\alpha + \phi_q(\alpha)q] \tag{31}$$

that is, ϕ_q scheduled with α instead of q (assuming that scheduling with α is possible). Continuation gives the required relationships, that is, the gains are calculated at each trim point so that they have a set of trimmed states associated with them as well as the single input parameter. The elements of the Jacobian matrix of the μ-scheduled system are then equated to those of the state-scheduled system:

$$\partial\dot{\delta}_e/\partial\alpha = 30K_\alpha = 30\Big[\phi_\alpha + (\partial\phi_\alpha/\partial\alpha)\alpha + (\partial\phi_q/\partial\alpha)q\Big] \tag{32}$$

$$\partial\dot{\delta}_e/\partial q = 30K_q = 30[\phi_q(\alpha)] \tag{33}$$

$$\partial\dot{\delta}_e/\partial\delta_e = -30 = -30 \tag{34}$$

Hence, the transformation set becomes

$$K_\alpha = \phi_\alpha(\alpha) + (\partial\phi_\alpha/\partial\alpha)\alpha + (\partial\phi_q/\partial\alpha)q \tag{35}$$

$$K_q = \phi_q(\alpha) \tag{36}$$

It is then possible to find ϕ_α using Eq. (20) because $\partial\phi_q/\partial\alpha$ can be determined numerically as a result of Eq. (36).

The benefits of this type of dynamic gain schedule will depend on the system. In general, a better-performing system than the parameter-scheduled one will result, but an inferior response when compared with the conventional transformation is likely. The reason for this lies in the inherent smoothing performed by the transformation of a schedule from static to dynamic due to the integration of the static gain schedule with respect to the feedback state. This results in the magnitude of the feedback signal to the actuator at off-trim points being less than it would have been with the untransformed schedule, and so actuator movement is reduced, leading to less dramatic transient motion. The modified transformation will smooth at least one less schedule than the conventional transformation, hence the system gains, although scheduled with a fast state and having the desired eigenvalues may retain many large variations in the system gains with the scheduling state.

To distinguish this situation from the one in Sec. II.A the following two types of DGS are defined:

1) Full dynamic gain schedule (F-DGS): a dynamic gain schedule created by transforming a static gain schedule with the feedback state.

2) Modified dynamic gain schedule (M-DGS): a dynamic gain schedule created by transforming at least one static gain schedule with a state other than the feedback state.

The implications of M-DGS in terms of response degradation relative to F-DGS are discussed in Sec. V.

C. General Result for the Transformation of Static-to-Dynamic Gain Schedules

Therefore, for a system of the form

$$\begin{aligned}
\dot{x}_1 &= f_1(x_1 \cdots x_n)\\
\dot{x}_2 &= f_2(x_1 \cdots x_n)\\
&\vdots\\
\dot{x}_{n-1} &= f_{n-1}(x_1 \cdots x_n)\\
\dot{x}_n &= -30x_n + 30[K_1(\mu)x_1 + \cdots + K_{n-1}(\mu)x_{n-1}]
\end{aligned} \tag{37}$$

the general transformation set is given by

$$K_{a_i}(\mu) = \phi_{a_i}(a_i) + \frac{\partial\phi_{a_i}}{\partial a_i}a_i + \sum_{j=1}^{b_n} a_{\text{flag}}\frac{\partial\phi_{b_j}}{\partial a_i}b_j\bigg|_{i=1,a_n} \tag{38}$$

$$K_{b_i}(\mu) = \phi_{b_i}(a_{\text{aux}_i})|_{i=1,b_n} \tag{39}$$

where

$\boldsymbol{a} \in \Re^{a_n}$ = vector of feedback states that can be used to schedule the associated feedback gain

$\boldsymbol{b} \in \Re^{b_n}$ = vector of the remaining feedback states

$\boldsymbol{a}_{\text{aux}} \in \Re^{b_n}$ = vector of states against which ϕ_{b_i} is scheduled

and where a_{flag} is defined as

$$a_{\text{flag}} = \begin{cases} 1 & a_i = a_{\text{aux}_j} \\ 0 & a_i \neq a_{\text{aux}_j} \end{cases} \tag{40}$$

III. Linear Quadratic State-Feedback Regulation

Previous work on continuation-based state-feedback dynamic gain scheduling [1,7] has exclusively used eigenstructure assignment to design the parameter-scheduled gains from which the state-scheduled gains are calculated. The eigenstructure was assigned in order that the system just satisfied level 1 handling qualities, for

example, the poles associated with the short period mode were placed at $-2 \pm 2i$. However, when the desired eigenstructure is not well defined, such as with a UCAV where requirements on handling qualities are not specified, the placing of the system poles to satisfy piloted handling qualities might be inappropriate. It could result in large feedback gains and, hence, in excessive effector deflections, possibly leading to actuator saturation and an increase in the radar cross-sectional signature. A much better way of selecting the closed-loop gains would be to use an approach that optimizes the system for the specific requirements of the given aircraft. LQR [14,23] is one such method, and the intrinsic MATLAB function *lqr* was used to calculate the controller for the work presented in this paper. Consider the state-space system

$$\dot{\hat{\boldsymbol{x}}} = \boldsymbol{A}\hat{\boldsymbol{x}} + \boldsymbol{B}\hat{\boldsymbol{u}} \tag{41}$$

$$\hat{\boldsymbol{y}} = \boldsymbol{C}\hat{\boldsymbol{x}} + \boldsymbol{D}\hat{\boldsymbol{u}} \tag{42}$$

The optimal control problem is to find a control vector $\boldsymbol{u}$ that drives the initial state vector $\boldsymbol{x}(0)$ to the desired final state vector $\boldsymbol{x}(\infty)$ while minimizing a performance index of the form

$$\boldsymbol{J}(\boldsymbol{u}) = \int_0^\infty g(\boldsymbol{x}, \boldsymbol{u}, t)\mathrm{d}t \tag{43}$$

The most useful functional form of this equation is a quadratic performance index:

$$\boldsymbol{J}(\boldsymbol{u}) = \int_0^\infty (\boldsymbol{x}^T\boldsymbol{C}^T\boldsymbol{Q}\boldsymbol{C}\boldsymbol{x} + \boldsymbol{u}^T\boldsymbol{R}\boldsymbol{u})\,\mathrm{d}t \tag{44}$$

where $\boldsymbol{Q}$ and $\boldsymbol{R}$ are weighting matrices that enable a tradeoff of regulation performance [i.e., how fast $\boldsymbol{x}(t)$ goes to zero] and control energy expenditure. For simplicity, the $\boldsymbol{R}$ matrix is set equal to the identity matrix for all the work presented here.

For these investigative design purposes, the LQR design constraints were chosen to give similar response characteristics (in terms of damping ratio and undamped natural frequency) to a system designed with level 1 handling quality requirements in mind, that is, a response similar to one that would be acceptable on a manned aircraft. A more systematic approach [24] might be to define maximum allowable deviations in $\boldsymbol{x}$ and $\boldsymbol{x}_{\max}$ and then set

$$\boldsymbol{Q} = \mathrm{diag}\{1/\boldsymbol{x}_{\max}^2\}$$

IV. Continuation Tailoring

Continuation tailoring [25–27] refers here to the use of bifurcation analysis in the shaping of bifurcation diagrams. Bifurcation diagrams (as used in this paper) show the variation of fixed points of a dynamic system (and their local stability) as the continuation parameter μ is varied. Fixed points, or equilibria, are points in state space where all time derivatives are zero. They are found by solving $\boldsymbol{f}(\boldsymbol{x}, \boldsymbol{\delta}) = 0$, where $\boldsymbol{f}$ is a nonlinear function that describes the aircraft in terms of the states $\boldsymbol{x}$ and the input parameters $\boldsymbol{\delta}$ (μ is an element of $\boldsymbol{\delta}$). A bifurcation diagram is a two-dimensional projection of equilibria values of a state variable plotted against the continuation parameter (a so-called one-parameter bifurcation diagram). In general, for open-loop systems, there will be multiple equilibria branches (e.g., spin steady states). The local stability of the fixed points is indicated by line type. Figure 3 is a bifurcation diagram in α of the open-loop model used in Sec. V.A. It shows the effector angle required to trim the aircraft at each α. The solid line indicates stable equilibria whereas the dashed line indicates unstable equilibria; the cause of the instability in the region $10\ \mathrm{deg} \leq \alpha \leq 12\ \mathrm{deg}$ is positive pitch stiffness.

In this paper, continuation tailoring specifically involves the shaping of a closed-loop bifurcation diagram to obtain a required steady-state relationship between one of the states and the continuation parameter. This is accomplished by utilizing an extra control input with the system in question. The ordinary differential equation (ODE) associated with the state that it prescribes is then solved for the value of the extra control input pseudocontinuously across the parameter input range using continuation methods. The result of this is a variation in the extra control input with the continuation parameter that moves the state in question to its prescribed trim value. This is then used as a feedforward (FF) gain schedule in time simulations to achieve the desired system behavior. For example, an additional signal (as a function of μ) could be applied to the pitch thrust vectoring input of the open-loop model in Fig. 3 to modify the relationship between PFact and α. It is seen in Sec. V that when the gains associated with the CAS integrator are transformed (for use in a DGS), then the trim values can change (unless there is full-authority control); additional control inputs (calculated via continuation tailoring) can be used to return the trim points to their original values.

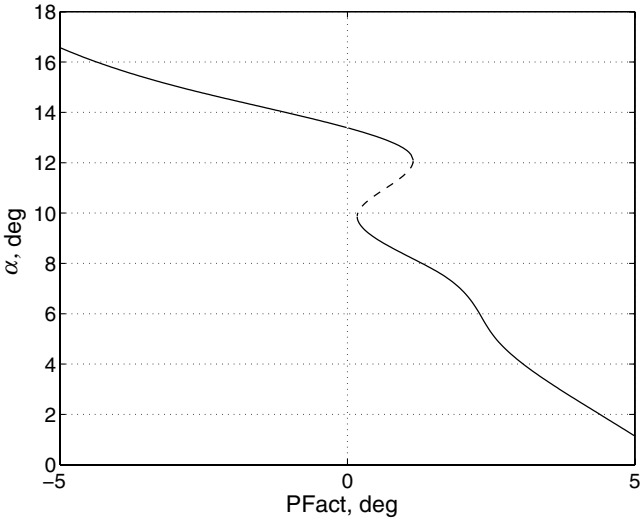

Fig. 3 Open-loop bifurcation diagram with μ = PFact.

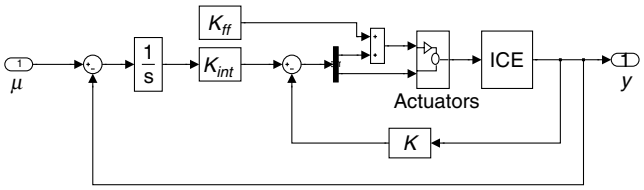

Fig. 4 Generic SCAS controller structure $+K_{ff}$.

In general, controller design using the DGS methodology involves the following steps: a) design of a classical gain schedule (CGS); b) transformation to a dynamic gain schedule to enable scheduling with a fast-varying state; and c) if the steady states are altered by the transformation, then a set of gains $K_{ff}(\mu)$ is calculated that can return the steady state to the original CGS closed-loop equilibrium position, that is, it provides the additional moments that are required to shift the equilibrium point. This is done by solving the ODE for a control effector input K_{ff} instead of the associated state. This additional signal could go to an effector already in use (as in Fig. 4) or it could be fed to a previously unused effector (if control effector redundancy exists).

V. UCAV Application

DGS control is now assessed using three versions of the ICE model. They have been given numbers for ease of reference and are defined in Table 1. Each has a full state-feedback stability

Table 1 ICE model version definitions

	Aircraft states	Actuators	CAS	Order
version 1	α, q	PF	α_{dem}	4th
version 2	α, β, p, q, r	δ_{yaw}, PF, AMTL	β_{dem}	9th
version 3	α, β,p, q, r	δ_{yaw}, PF, AMTL	α_{dem}, β_{dem}	10th

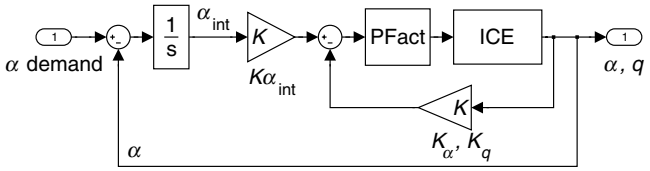

Fig. 5 Block diagram of the ICE (version 1).

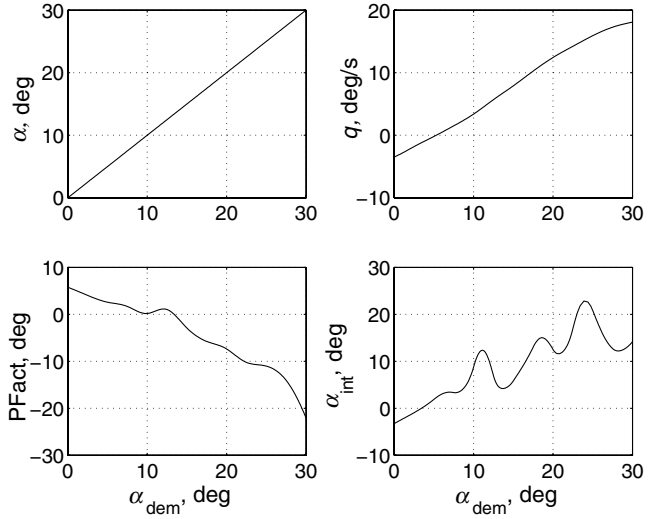

Fig. 6 Bifurcation diagrams for the ICE (version 1).

augmentation system (SAS) and at least one outer command loop. The actuators have been modeled by simple first-order lags of the form $30/(s + 30)$ with position saturation limits only.

The closed-loop systems were incorporated into the continuation software [22] with the gains being calculated directly for each trim point using LQR. Output feedback controllers are calculated in each case considered here. It is assumed that all states are either measurable or can be estimated (and are hence available for feedback) apart from the actuator position states. Continuation methods allow trim points to be calculated pseudocontinuously across a parameter space. At each point, the system is linearized and a set of controller gains calculated. Hence, trimming and controller design are done together. This yields a controller that will provide near optimum control for all trim points throughout the parameter space. By calculating the controller gains in this way, the underlying physics of the system can be retained through the bifurcation diagrams, and it is possible to examine all of the states (including the controller states) at each trim point.

Continuation methods are the primary tool of bifurcation analysis that has been used extensively to analyze and modify aircraft dynamics [15,28–30]. No bifurcations will be present in the closed-loop work as the command augmentation system will provide a single stable trim branch throughout the given parameter space, though these trim maps are still referred to as bifurcation diagrams.

For the purposes of assessing the effectiveness of DGS control, ideal systems are defined as benchmarks. They are ideal because they consist of simple transfer functions that have unity gain and the same roots as the LQR closed-loop system.

A. Fourth-Order Model (Version 1)

Figure 5 shows the first version of the model to be tested. The $\boldsymbol{Q}$ and $\boldsymbol{R}$ matrices for the runs in this section were

$$\boldsymbol{Q} = \begin{bmatrix} 0 & 0 & 0 \\ 0 & 0 & 0 \\ 0 & 0 & 20000 \end{bmatrix} \tag{45}$$

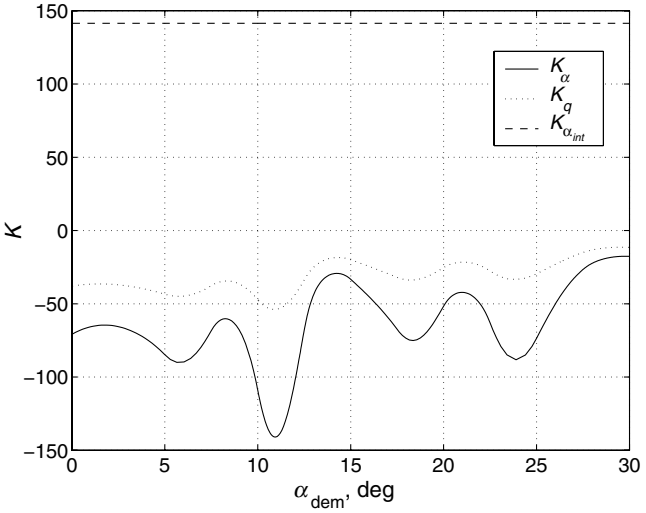

Fig. 7 Static gain variations with the continuation parameter α_{dem}.

$$\boldsymbol{R} = [1] \tag{46}$$

The MATLAB *lqr* routine was used to calculate an optimum controller of the form $u = -\boldsymbol{K}\boldsymbol{x}$, where $\boldsymbol{x} = [\alpha, q, \alpha_{\text{int}}]$, pseudo-continuously across the continuation parameter range.

The bifurcation diagrams for this run are given in Fig. 6. The continuation parameter limits were defined arbitrarily to be $0\,\text{deg} \leq \alpha_{\text{dem}} \leq 30\,\text{deg}$ to allow a reasonable test range, and this range is achievable using the pitch flap actuator. The nonlinearity of the underlying system is indicated by the integrator state variation. Note that a reduced-order flight mechanics model such as this, where slow modes are neglected, ignores variation of gravitational loads with aircraft attitude and results in trims with nonzero pitch rate.

The variation of the static gains with α_{dem} are shown in Fig. 7. The CAS integrator is invariant with the continuation parameter, and so only two gains need to be converted; and F-DGS is possible because these gains are single valued at each α_{dem} and have values at $\alpha_{\text{dem}} = 0$. Hence, the static gain schedule was transformed to a F-DGS using the following transformation set:

$$K_\alpha = \phi_\alpha + [(\partial\phi_\alpha/\partial\alpha)\alpha] \tag{47}$$

$$K_q = \phi_q + [(\partial\phi_q/\partial q)q] \tag{48}$$

The transformed gain variation is plotted with the original static gains in Fig. 8. It shows the static and dynamic gains to be equal at certain points, that is, $K_\alpha(\alpha_{\text{dem}}) = \phi_\alpha(\alpha)$ when $\alpha = 0$ and when $\partial\phi_\alpha/\partial\alpha = 0$ [as expected from Eq. (19)]. Similarly, it shows that $K_q(\alpha_{\text{dem}}) = \phi_q(q)$ when $q = 0$ and when $\partial\phi_q/\partial q = 0$. Note also that the dynamic gains are necessarily smoother than the static.

Step inputs were then applied to test the validity of the F-DGS. A comparison of the response to a step input in α_{dem} of 4 deg (from an initial trim at $\alpha = 11$ deg) is shown in Fig. 9. This step input was chosen to ensure that a highly nonlinear region in the gain variation with α was encountered (see Fig. 8). The F-DGS response is superior in terms of both proximity to the ideal response and in terms of the

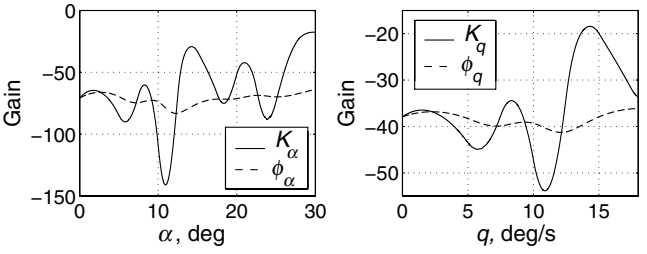

a) α feedback gain **b) q feedback gain**

Fig. 8 Static and dynamic gain variations for $0\,\text{deg} \leq \alpha_{\text{dem}} \leq 30\,\text{deg}$.

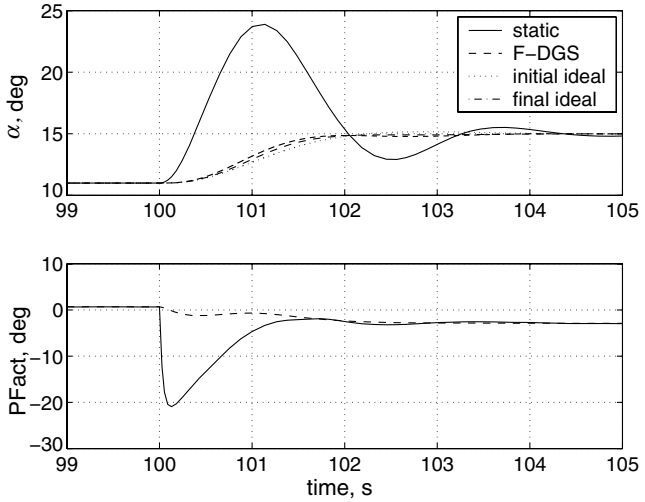

Fig. 9 Response to a step in α_{dem} of 4 deg away from trim.

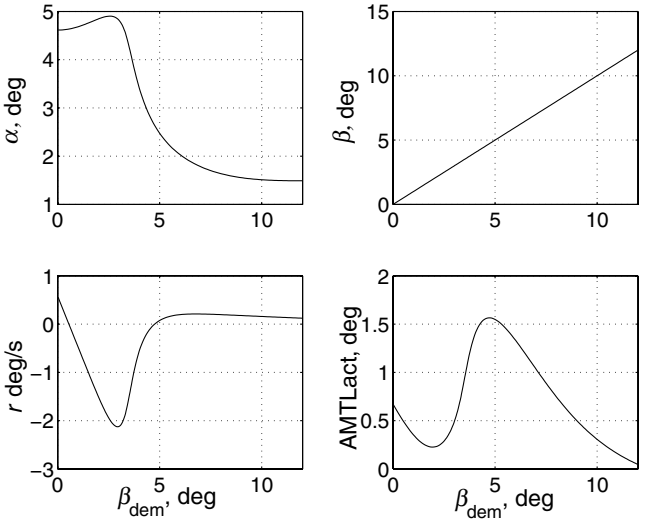

Fig. 11 Bifurcation diagrams in the range 0 deg $\leq \beta_{\text{dem}} \leq$ 12 deg.

much smaller pitch flap actuator movement. There are two ideal responses shown in Fig. 9 because the stability at the initial trim condition and that at the end will be different. In fact, the stability will be constantly changing, and so it was decided to plot the ideal responses as defined by the eigenvalues at the pre- and post-step trims. The F-DGS system response was observed over a number of trials to be consistently much closer to the ideal ones than to the parameter-scheduled (static) system.

B. Ninth-Order Model (Version 2)

Figure 10 shows the second version of the model to be tested, where $\boldsymbol{K}_i$ is a vector of gains $(K_{\alpha_i}, K_{\beta_i}, K_{p_i}, K_{q_i}, K_{r_i})$ that is multiplied by the feedback state vector.

The LQR design constraints were chosen to be:

$$\boldsymbol{Q} = \begin{bmatrix} 10000 & 0 & 0 & 0 & 0 & 0 \\ 0 & 0 & 0 & 0 & 0 & 0 \\ 0 & 0 & 0 & 0 & 0 & 0 \\ 0 & 0 & 0 & 10000 & 0 & 0 \\ 0 & 0 & 0 & 0 & 0 & 0 \\ 0 & 0 & 0 & 0 & 0 & 40000 \end{bmatrix} \tag{49}$$

$$\boldsymbol{R} = \begin{bmatrix} 1 & 0 & 0 \\ 0 & 1 & 0 \\ 0 & 0 & 1 \end{bmatrix} \tag{50}$$

for a control law of the form $\boldsymbol{u} = -\boldsymbol{K}\boldsymbol{x}$, where $\boldsymbol{x} = [\alpha, \beta, p, q, r, \beta_{\text{int}}]$. Here the $\boldsymbol{Q}$ matrix requires a fast response in β_{dem} and in the longitudinal short period mode. This was done to reduce the longitudinal/lateral system coupling, which, in turn, allowed the ideal system to be identified more easily and mimic the way in which the eigenstructure assignment was constrained in previous work [17]. Hence, the elements of the eigenvectors associated with α and q in the lateral modes are minimal.

Figure 11 shows the bifurcation diagrams for this system with β_{dem} set as the continuation parameter. The β_{dem} range was chosen arbitrarily so as to allow a fair assessment of the model.

The functions relating trimmed α, p, q, and r to their associated static feedback gains were not all one-to-one or many-to-one: see Fig. 12, where the variations in these gains, fed back to their respective actuators, are plotted with respect to their equilibria feedback states. A modified transformation set was therefore used to convert the static gain schedule to an M-DGS, namely

$$K_\alpha = \phi_\alpha(\beta) \tag{51}$$

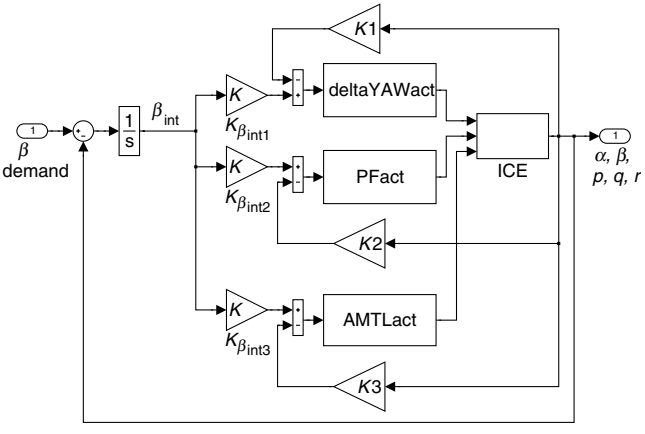

Fig. 10 Block diagram of the ICE (version 2).

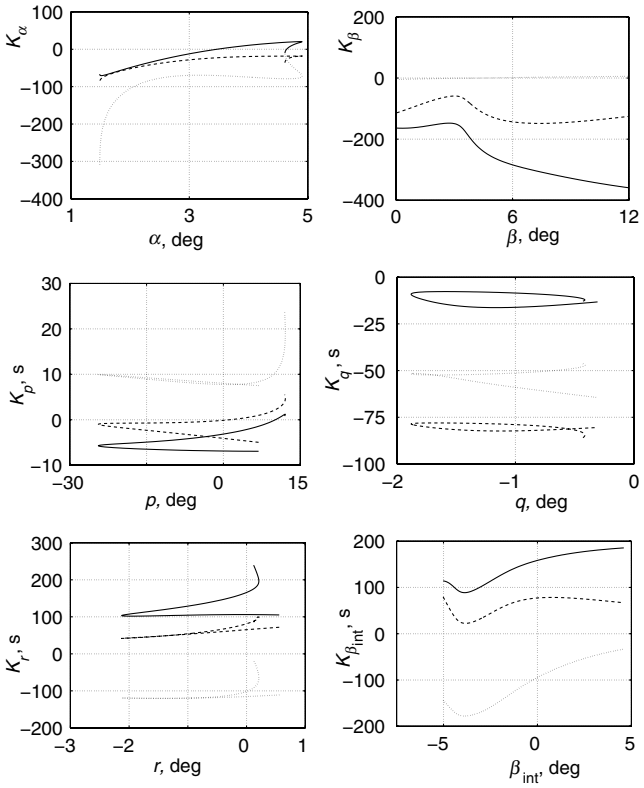

Fig. 12 Variation in static gains with feedback states (solid, δ_{yaw}; dashed, PF; dotted, AMTL).

$$K_\beta = \phi_\beta(\beta) + [(\partial\phi_\beta/\partial\beta)\beta] + [(\partial\phi_\alpha/\partial\beta)\alpha] + [(\partial\phi_p/\partial\beta)p] + [(\partial\phi_q/\partial\beta)q] + [(\partial\phi_r/\partial\beta)r] \quad (52)$$

$$K_p = \phi_p(\beta) \quad (53)$$

$$K_q = \phi_q(\beta) \quad (54)$$

$$K_r = \phi_r(\beta) \quad (55)$$

$$K_{\beta_{\text{int}}} = \phi_{\beta_{\text{int}}}(\beta_{\text{int}}) + [(\partial\phi_{\beta_{\text{int}}}/\partial\beta_{\text{int}})\beta_{\text{int}}] \quad (56)$$

Although no direct comparisons can be made because the static gains are optimized for the three-effector system, the reason for the folds in the gain variations with the feedback states can be explained by the presence of fold bifurcations in the open-loop system with the left AMT actuator (AMTLact) as the continuation parameter (as shown in Fig. 13). The continuation parameter range was chosen to reflect the movement of AMTLact in the closed-loop system.

Figure 14 compares the variation in the static and dynamic gains with the associated feedback state. The β subfigures do not conform to the standard requirement of K_β equalling ϕ_β for $\beta = 0$ and $\partial\phi_\beta/\partial\beta = 0$, as there are extra terms in the equation that defines K_β (52). Hence, the gain-smoothing effect is negligible in this case, as the transformed dynamic gain variations are only slightly smoother than the original static gains.

The conversion to a dynamic gain, though retaining the eigenvalues of the system, does in fact alter many of the steady states, that is, the bifurcation diagram trim branches will change. As the controllers are only valid at the designed trim points, then the stability will also change. A comparison of the μ-scheduled and state-scheduled (M-DGS) closed-loop bifurcation diagrams is shown in Figs. 15 and 16. The steady-state differences are small, up to $\beta_{\text{dem}} = 3$ deg, but quickly become significant for large demands. This byproduct of modified dynamic gain schedule transformation is addressed in Sec. V.D using continuation tailoring.

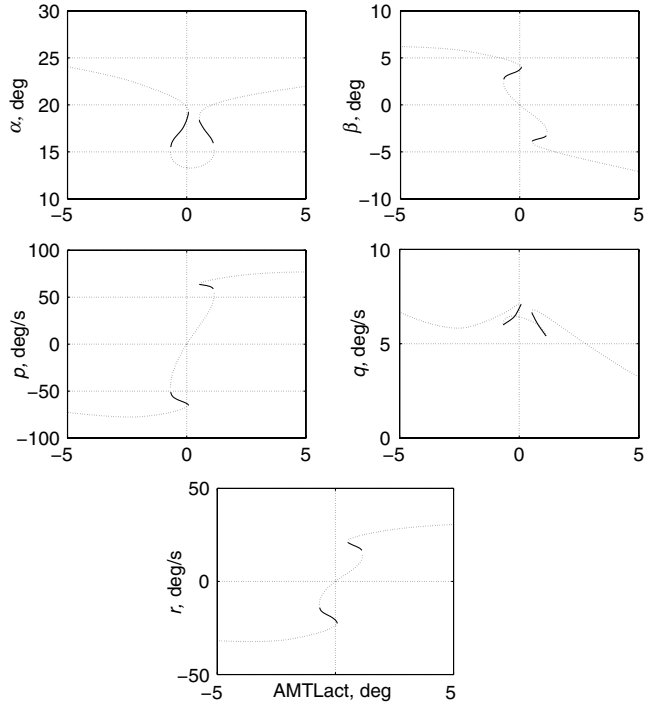

Fig. 13 Open-loop bifurcation diagrams for μ=AMTLact (solid line, stable; dotted line, unstable).

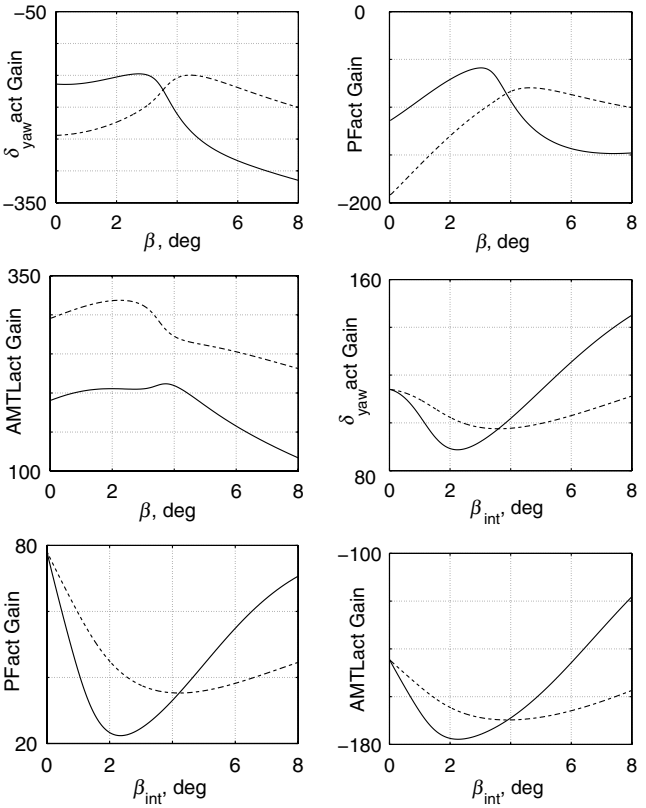

Fig. 14 Gains that are fed back to δ_{yaw}act (solid line, K; dashed line, ϕ).

C. Tenth-Order Model (Version 3)

The third version of the model to be investigated is identical to the second (version 2), aside from it having an additional α-demand outer command loop.

The $\boldsymbol{Q}$ matrix is also the same as the one applied to the control of the second model, apart from an additional row and column for the α_{int} state, which consists entirely of zeros, apart from the leading diagonal α_{int} penalty, which is set at 10,000. The $\boldsymbol{R}$ matrix is the same as that used in the previous section.

The same control law structure is also used, that is, $\boldsymbol{u} = -\boldsymbol{K}\boldsymbol{x}$ with $\boldsymbol{x} = [\alpha, \beta, p, q, r, \beta_{\text{int}}, \alpha_{\text{int}}]$. Hence, the desired controller provides a good deal of longitudinal/lateral mode decoupling and demands a sharper response in β than in α. Note that this system is merely an example for the purpose of demonstrating the gain-scheduling

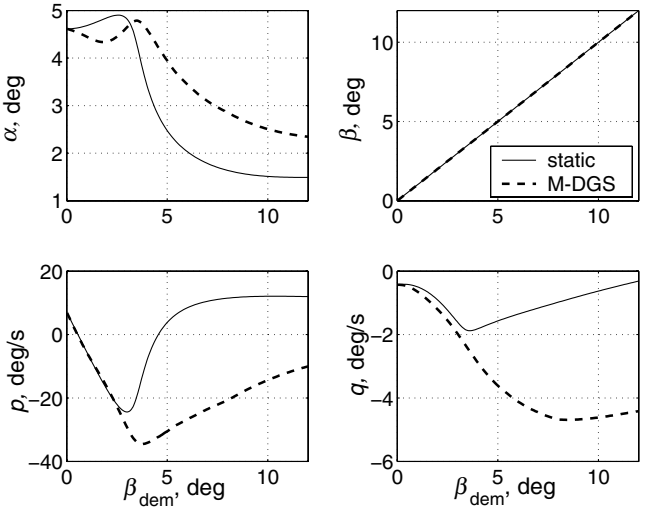

Fig. 15 M-DGS and μ-scheduled system bifurcation diagrams: α, β, p, and q.

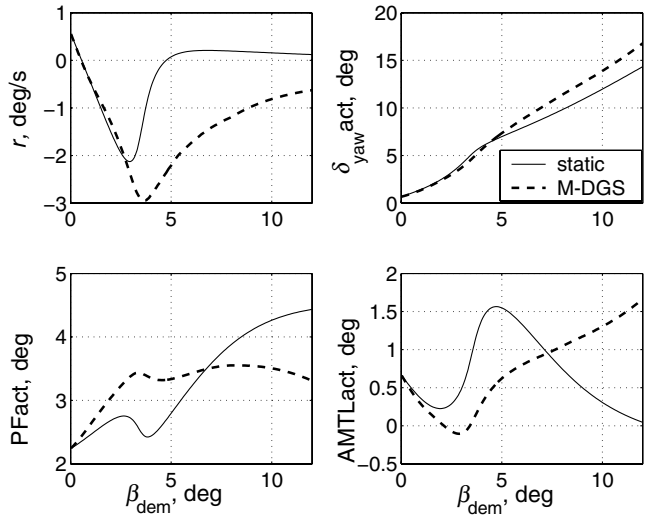

Fig. 16 M-DGS and μ-scheduled system bifurcation diagrams; r and actuator states.

approach that is advocated. In reality, it would be desirable to have control over roll rate too, via an additional p-demand CAS loop.

Two-parameter trim maps were obtained by setting the α_{dem} input to a particular value and then holding it constant while a continuation run was carried out with β_{dem} as the continuation parameter in the range $0\,\text{deg} \le \beta_{\text{dem}} \le 10\,\text{deg}$. This was done for α_{dem} in the range -5 to 5 deg in steps of 1 deg. Two-parameter trim maps were then obtained by concatenating the 11 separate runs. A selection of them is shown in Fig. 17.

Similar plots are possible for the gain variations, but there would be 21 of them (7 gains going to 3 actuators), and so they are omitted for brevity. An F-DGS was not possible, as most of the static gain variations with β (at each α) were neither one-to-one nor many-to-one functions. Hence, an M-DGS was created by applying the following transformation set to the gain variation with β_{dem} at each of the 11 α_{dem} values and then concatenating the M-DGS:

$$K_\alpha(\alpha_{\text{dem}}, \beta_{\text{dem}}) = \phi_\alpha(\alpha_{\text{dem}}, \beta) \tag{57}$$

$$\begin{aligned} K_\beta(\alpha_{\text{dem}}, \beta_{\text{dem}}) \quad &= \phi_\beta(\alpha_{\text{dem}}, \beta) + [(\partial\phi_\beta/\partial\beta)\beta] + [(\partial\phi_\alpha/\partial\beta)\alpha] \\ &+ [(\partial\phi_p/\partial\beta)p] + [(\partial\phi_q/\partial\beta)q] + [(\partial\phi_r/\partial\beta)r] \\ &+ [(\partial\phi_{\alpha_{\text{int}}}/\partial\beta)\alpha_{\text{int}}] + [(\partial\phi_{\beta_{\text{int}}}/\partial\beta)\beta_{\text{int}}] \end{aligned} \tag{58}$$

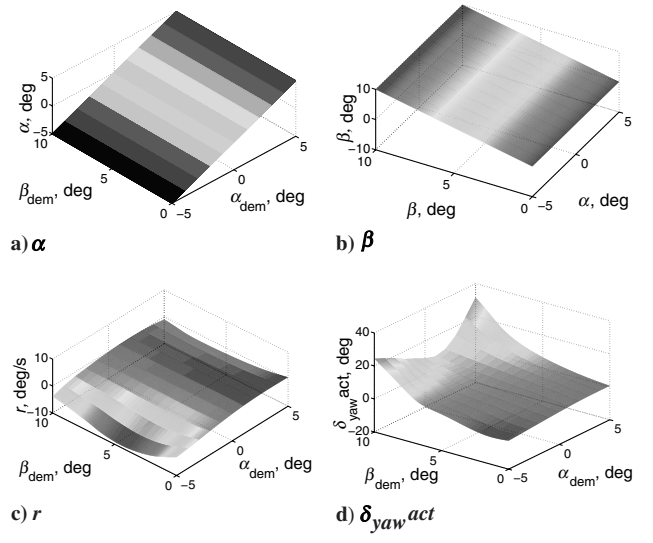

Fig. 17 Two-parameter trim maps for α, β, r, and δ_{yaw}act.

$$K_p(\alpha_{\text{dem}}, \beta_{\text{dem}}) = \phi_p(\alpha_{\text{dem}}, \beta) \tag{59}$$

$$K_q(\alpha_{\text{dem}}, \beta_{\text{dem}}) = \phi_q(\alpha_{\text{dem}}, \beta) \tag{60}$$

$$K_r(\alpha_{\text{dem}}, \beta_{\text{dem}}) = \phi_r(\alpha_{\text{dem}}, \beta) \tag{61}$$

$$K_{\alpha_{\text{int}}}(\alpha_{\text{dem}}, \beta_{\text{dem}}) = \phi_{\alpha_{\text{int}}}(\alpha_{\text{dem}}, \beta) \tag{62}$$

$$K_{\beta_{\text{int}}}(\alpha_{\text{dem}}, \beta_{\text{dem}}) = \phi_{\beta_{\text{int}}}(\alpha_{\text{dem}}, \beta) \tag{63}$$

The pure parameter-scheduled (α_{dem} and β_{dem}) system response is compared with the mixed M-DGS/parameter-scheduled (β and α_{dem}) system response in Fig. 18 by applying a simultaneous step input in α_{dem} and β_{dem} of 3 and 5 deg, respectively. It shows a comparison of the system response in the tracked states (i.e., α and β).

Finally, Fig. 19 shows a comparison of the tracked state responses to a more demanding combination of simultaneous step inputs in α_{dem} and β_{dem}. Hence, scheduling with two variables (one parameter and one fast state) is shown to give a better response than scheduling with two parameters.

D. Continuation Tailoring

Figures 15 and 16 highlight a byproduct of transforming the gain schedule from parameter-scheduled to either F-DGS or M-DGS. Its effect only becomes apparent in regions where the two trim curves (i.e., static and dynamic schedules) are far from each other (such as at $\beta_{\text{dem}} = 10\,\text{deg}$ in this figure, which is a fairly extreme demand). The original gain schedule is calculated for a given set of trim points. When the transformations are carried out, the eigenstructure of the system is retained but the trim values are not. As the eigenstructure only characterizes desired behavior at trims corresponding to the static schedule design case, this divergence of the trim branches will therefore result in a change in the desired stability (away from that which gives an optimum response) at the dynamic gain schedule trim point.

It is proposed that a feedforward gain schedule K_{ff} (applied to the system as shown in Fig. 4) be used to retain the values of the trim states of the system after the static gain schedule has been transformed to a dynamic one. This compensation schedule is designed using continuation tailoring. In order that the method be demonstrated, a slice of the two-parameter gain schedule at $\alpha_{\text{dem}} = 0\,\text{deg}$ in Sec. V.C is considered. Figure 20 compares the β_{dem}-scheduled system with the M-DGS system at $\alpha_{\text{dem}} = 0\,\text{deg}$. The trims are identical in the demanded states α and β but different in all the other states (of which only p and AMTLact are shown here for

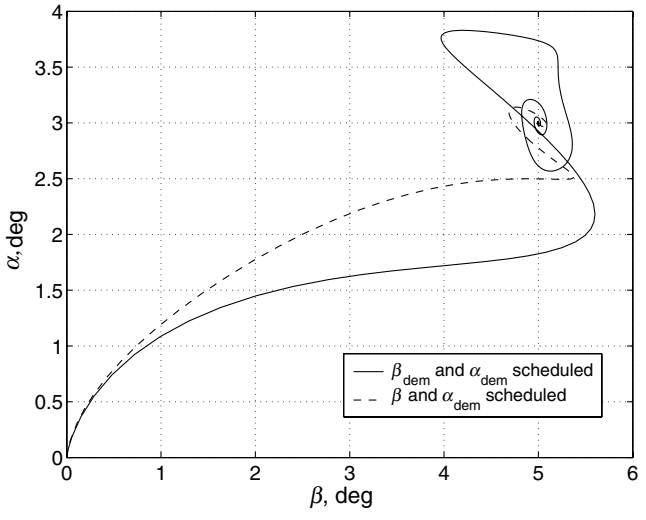

Fig. 18 Response to step inputs of 5 deg in β_{dem} and 3 deg in α_{dem}.

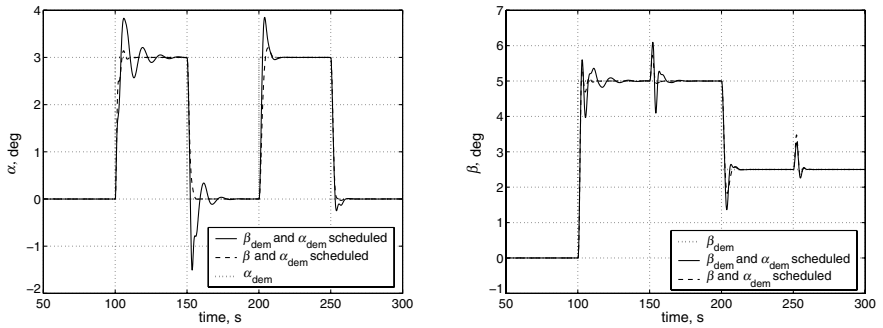

a) α b) β

Fig. 19 Step input tracking response to demands in both α and β.

brevity). The trims are fairly close for $\beta_{\text{dem}} \leq 6$ deg but start to diverge rapidly with increasing β_{dem}.

If there were a three-axis demand system, for example, q_{dem}, β_{dem}, and p_{dem}, then the steady states would in practice be identical for all values in parameter space. More generally, the steady states are only different when the number of command integrators is less than the number of unconstrained axes.

The feedforward gain schedule is obtained by solving the $\dot{p}$ equation for the required feedforward gain to give the same trimmed p as would have been obtained with the static gain schedule within the continuation design framework. This feedforward gain schedule is shown in Fig. 21. Hence (as intuitively expected) K_{ff} is relatively large in the region where the static and dynamic scheduled system trims are furthest apart.

Figure 22 compares the β response to a step in β_{dem} of 7 deg (i.e., a value where the trims are significantly altered by DGS). It also shows the parameter-scheduled response. The dynamic schedule for large step inputs where the two trims are vastly different are inferior unless the feedforward term is used, as the stability is only optimum for the designed static trim.

Note that the disturbance rejection properties are not recovered by the addition of the feedforward signal, and so caution must be exercised if such a controller structure is required. A recommended implementation of DGS may therefore only transform the SAS gains and retain the parameter-scheduled CAS gain to negate the need for the additional feedforward signal.

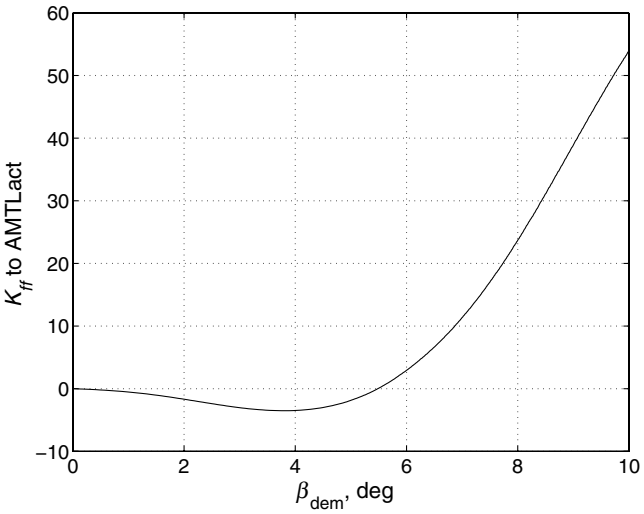

Fig. 21 Feedforward schedule that returns closed-loop trims to their static schedule values.

V. Conclusion

In this paper a method for scheduling gains against rapidly changing states has been applied to an unmanned combat air vehicle model. The dynamic gains were determined directly by applying a transformation to static gain schedules that were themselves calculated pseudocontinuously from within a continuation design framework using linear quadratic regulation.

The method is shown to significantly improve the transient response for both longitudinal and longitudinal/lateral versions of the model when stepping between trim conditions.

The problem of control surface position limit saturation has also been shown to be less likely when a full dynamic gain schedule is used; this is because the magnitude range of the gains is smaller than that of the original static gains, as a result of the transformation process. F-DGS transformation was found to have the additional

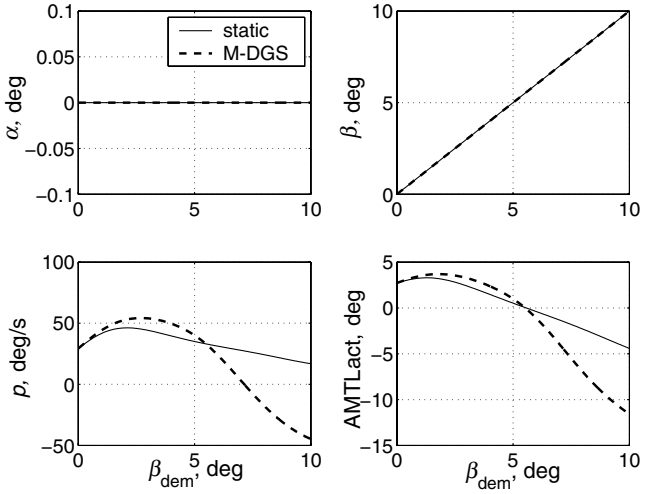

Fig. 20 A selected comparison of the static and dynamic gain-scheduled system trim branches.

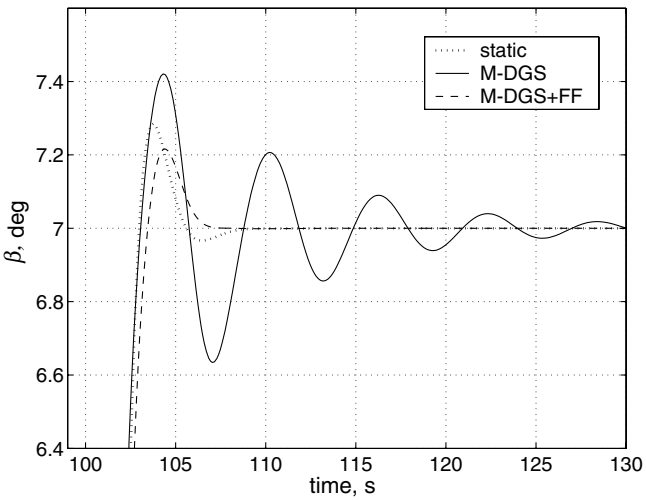

Fig. 22 The comparative response in β to a step in β_{dem} of 7.0 deg

benefit of smoothing the highly nonlinear gain variation. Both of these advantages are likely but not necessarily realized with modified DGS. The addition of a feedforward gain schedule was shown to be necessary when applying DGS to systems without full-authority integral control.

Although this continuation-based design methodology requires knowledge of nonlinear systems theory, it retains a strong link to the underlying physics via the bifurcation diagrams and, hence, gives the user a much deeper insight into the behavior of both the open and closed-loop systems than conventional black-box approaches, for example, the actuator states that are required to trim the aircraft at a given point provide a measure of the control power expenditure and availability, the variation of control system integrator states indicates the extent of system nonlinearities, and the local stability of linearizations of the nonlinear system can be used to predict global behavior.

This paper has advanced the method with the addition of modified static-to-dynamic gain schedule transformations. This allowed its extension to a longitudinal/lateral aircraft model by proposing a means of designing dynamic gain schedules when multivalued behavior arises in nonlinear systems.

Acknowledgment

The supply of data for the ICE 101-TV model by the Air Force Research Laboratory at Wright-Patterson Air Force Base is gratefully acknowledged.

References

[1] Richardson, T., Davison, P., Lowenberg, M., and di Bernardo, M., "Control of Nonlinear Aircraft Models Using Dynamic State-Feedback Gain Scheduling," AIAA Paper 2003-5503, Aug. 2003.

[2] Rugh, W., and Shamma, J., "Research on Gain Scheduling," *Automatica: The Journal of IFAC, the International Federation of Automatic Control*, Vol. 36, No. 10, 2000, pp. 1401–1425.

[3] Leith, D., and Leithead, W., "Survey of Gain-Scheduling Analysis & Design," *International Journal of Control*, Vol. 73, No. 11, 2000, pp. 1001–1025.

[4] Apkarian, P., Gahinet, P., and Becker, G., "Self-Scheduled H_∞ Linear Parameter-Varying Systems," *Proceedings of the American Control Conference*, Vol. 1, IEEE Publications, Piscataway, NJ, 1994, pp. 856–860.

[5] Papageorgiou, G., Glover, K., D'Mello, G., and Patel, Y., "Taking Robust LPV Control into Flight on the VAAC Harrier," *Proceedings of the 39th IEEE Conference on Decision and Control*, Vol. 5, IEEE Publications, Piscataway, NJ, 2000, pp. 4558–4564.

[6] Nichols, R., and Reichert, R., "Gain Scheduling for *H*-Infinity Controllers: A Flight Control Example," *IEEE Transactions on Control Systems Technology*, Vol. 1, No. 2, 1993, pp. 69–79.

[7] Lawrence, D., and Rugh, W., "Gain Scheduling Dynamic Linear Controllers for a Nonlinear Plant," *Automatica : the Journal of IFAC, the International Federation of Automatic Control*, Vol. 31, No. 3, 1995, pp. 381–390.

[8] Rugh, W., "Analytical Framework for Gain Scheduling," *IEEE Control Systems Magazine*, Vol. 11, No. 1, 1991, pp. 79–84.

[9] Dorsett, K., and Mehl., D., "Innovative Control Eectors (ICE)," WL-TR-96-3043, January 1996.

[10] Dorsett, K., Fears, S., and Houlden, H., "Innovative Control Effectors (ICE) Phase II," Wright Laboratories, Rept. WL-TR-97-3059, WrightPatterson Air Force Base, 1997.

[11] Masey, J., "Unmanned Vehicles Handbook 2005," The Shephard Press, Burnham, England, 2004, pp. 85–89.

[12] Lowenberg, M., and Richardson, T., "The Continuation Design Framework for Nonlinear Aircraft Control," AIAA Paper 2001-4100, Aug. 2001.

[13] Tischler, M., Lee, J., and Colbourne, J., "Optimization and Comparison of Alternative Flight Control System Design Methods Using a Common Set of Handling-Qualities Criteria," AIAA Paper 2001-4266, 2001.

[14] Nelson, R., *Flight Stability and Automatic Control*, McGraw–Hill, New York, 1998, pp. 359–394.

[15] Lowenberg, M., "Application of Bifurcation Analysis to Multiple Attractor Flight Dynamics," Ph.D. Dissertation, University of Bristol, Bristol, England, Aug. 1998.

[16] Richardson, T., "Continuation Methods Applied to Nonlinear Flight Dynamics and Control," Ph.D. Dissertation, University of Bristol, Bristol, England, 2002.

[17] Jones, C., Richardson, T., and Lowenberg, M., "Dynamic State-Feedback Gain Scheduled Control of the ICE 101-TV," AIAA Paper 2004-4754, Aug. 2004.

[18] Andry, A., Shapiro, E., and Chung, J., "Eigenstructure Assignment for Linear Systems," *IEEE Transactions on Aerospace and Electronic Systems*, Vol. 19, No. 5, 1983, pp. 711–728.

[19] Sobel, K., Shapiro, E., and Andry, A., "Eigenstructure Assignment," *International Journal of Control*, Vol. 59, No. 1, 1994, pp. 13–37.

[20] Gibson, L., Nichols, N., and Littleboy, D., "Closed Loop Design for a Simple Non-Linear Aircraft Model Using Eigenstructure Assignment," AIAA Paper 1997-3779, Aug. 1997.

[21] Hyde, R., and Glover, K., "The Application of Scheduled H_∞ Controllers to a VSTOL Aircraft," *IEEE Transactions on Automatic Control*, Vol. 38, No. 7, 1993, pp. 1021–1039.

[22] Doedel, E., "AUTO 97: Continuation and Bifurcation Software for Ordinary Differential Equations," [online software manual], http://indy.cs.concordia.ca/auto/ [cited 1 Sep. 2002].

[23] Stevens, B. L., and Lewis, F. L., *Aircraft Control and Simulation*, Wiley, New York, 2003, pp. 403–484.

[24] Bryson, A., and Ho, Y., *Applied Optimal Control*, Hemisphere, Washington, D.C., 1975, pp. 148–176.

[25] Jones, C., "Dynamic Gain-Scheduled Control of a Nonlinear UCAV Model," Ph.D. Thesis, University of Bristol, Bristol, England, Nov. 2005.

[26] Wang, X., di Bernardo, M., Stoten, D., Lowenberg, M., and Charles, G., "Bifurcation Tailoring via Newton Flow-Aided Adaptive Control," *International Journal of Bifurcation and Chaos in Applied Sciences and Engineering*, Vol. 13, No. 3, 2003, pp. 677–684.

[27] Charles, G., di Bernardo, M., Lowenberg, M., Stoten, D., and Wang, X., "Bifurcation Tailoring of Equilibria: A Feedback Control Approach," *Latin American Applied Research*, Special Theme Issue, Bifurcation Control: Methodologies and Applications, Vol. 31, No. 3, 2001, pp. 199–210.

[28] Carrol, J., and Mehra, R., "Bifurcation Analysis of Nonlinear Aircraft Dynamics," *Journal of Guidance, Control, and Dynamics*, Vol. 5, No. 5, 1982, pp. 529–536.

[29] Avanzini, G., and de Matteis, G., "Bifurcation Analysis of a Highly Augmented Aircraft Model," AIAA Paper 1996-3367, July 1996.

[30] Jahnke, C., and Culick, F., "Application of Bifurcation Theory to the High-Angle-of-Attack Dynamics of the F-14," *Journal of Aircraft*, Vol. 31, No. 1, 1994, pp. 26–34.